Identification of smectites by IR and LIBS instruments of SuperCam Suite onboard Mars 2020 Perseverance rover: comments on the Non-retrieval of First Drill Core

Subham Sarkar[1,2], Narayan Bose[3,*], Satadru Bhattacharya[1,3] and Subhash Bhandari[2]

[1]Space Applications Centre (Indian Space Research Organization), Ahmedabad 380 015, India
[2]Department of Earth and Environmental Science, KSKV Kachchh University, Bhuj 370 001, India
[3]Department of Geology and Geophysics, Indian Institute of Technology Kharagpur, Kharagpur 721 302, India

Preliminary investigations on the Infrared Spectrometer onboard Mars 2020 Perseverance rover show the presence of Fe-/Mg-smectite minerals near the first drilling site, Roubion. Laser-Induced Breakdown Spectrometer data show characteristic emission peaks for O, H and the major constituent elements of smectites, viz. Si, Fe, Mg, etc. These minerals suggest aqueous alteration of the basaltic floor of the Jezero crater. The mechanically weak nature of this basalt weathering layer holds clues to the non-retrieval of the first drill core. Water confinement capacity and high porosity–permeability make the smectite-rich rock units a good host for preserving macro- and microscopic biosignatures.

Keywords: Biosignature, drill core, Jezero crater, rover, smectites, spectroscopic analysis.

WITH the primary focus to search for biosignatures and collect samples for Earth return, the Perseverance rover has landed on the Jezero crater (~18.4°N, 77.5°E), Mars, as a part of the Mars 2020 mission[1]. The geological diversity of this crater is reflected in the vis-à-vis existence of delta fan deposits, the volcanic floor of the crater and the impact breccias on its rim[2,3]. Whereas, here the search for biosignatures is influenced by the presence of fluvio-lacustrine sediments, especially carbonates[1,3,4]. Orbiter data from the Jezero crater have already shown the presence of mafic silicates, carbonates and opaline silica[3–6]. The rover has landed on the oldest (Noachian–Hesperian, >3 Ga) part of the crater, considered to be the remnant of the volcanic floor unit[3,7], which is also referred to as 'Crater Floor Fracture Rough' or 'Pavers stone'[8,9]. The SuperCam bundle onboard the rover is a suite of six instruments, namely visible (VIS) spectrometer and Infrared (IR) Spectrometer, Laser-Induced Breakdown Spectrometer (LIBS), Raman Spectrometer, Time-resolved Luminescence Spectrometer (TRLS) and Remote Micro Imager (RMI) camera along with an acoustic sensor[10,11]. The very first abrasion site (to expose the fresh surface), i.e. 'Guillaumes' as well as the first drilling site (for sample collection), i.e. 'Roubion' are located on the volcanic floor unit (18.427253°N, 77.451607°E)[12]. Surprisingly, the drill core could not be obtained owing to the unexpected friable nature of the sample. However, like other targets, the IR and LIBS data were obtained at this drilling site also. However, instead of collecting data from only the fresh exposure and abraded surface, they were also collected from this drill hole and dust pile created by the drilling process, thus providing IR and LIBS spectra from the martian subsurface. The aim of this study is to analyse these IR and LIBS data for a better understanding of the mineralogical configuration of this region. Previous works[13], based on Compact Reconnaissance Imaging Spectrometer for Mars (CRISM) instrument onboard the Mars Reconnaissance Orbiter (MRO), has indicated the presence of carbonate-bearing olivine and Fe-/Mg-smectite[3–5] along with localized occurrences of hydrated silica[6].

The detailed activity log along with the datasets are open to access via the Planetary Data System (PDS) Geosciences Node[14]. During sol 157–168 (1 sol = 1 Martian day), the rover stayed at a location (i.e. no 'drive') near 18.42769464°N, 77.45164982°E and explored the targets Lagne, Castillon, Grand Coyer, Mure, Guillaumes and Roubion (Table 1). In this study, the Calibrated Data Records (CDRs) are used for the analysis of IR and LIBS spectra. Figure 1 shows

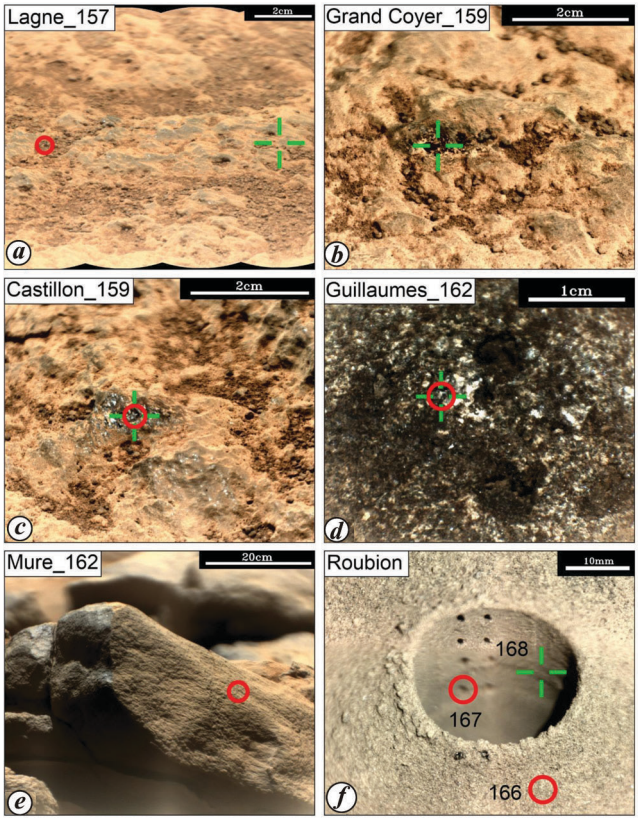

Figure 1. Remote Micro Imager images of the targets showing the data acquire points for the Infrared (IR) Spectrometer (red circle) and Laser-induced Breakdown Spectrometer (LIBS) (green crosshair) data.

*For correspondence. (e-mail: narayan.bghs@gmail.com)

Table 1. Details of six targets along with their representative data-point numbers (w.r.t. the PDS datasets[14]) for IR and LIBS data analysed

Target	Target property	Representative data [sol (point no.)] IR	LIBS
Lagne	Weathered surface	157 (10)	157 (1)
Grand Coyer		–	159 (10)
	Castillon	159 (9)	
Guillaumes	Abraded surface	162 (3)	
Mure	Weathered surface	162 (1)	–
Roubion	Drill cutting	166 (2)	–
	Drill hole	167 (7)	168 (1)

the RMI photographs of these targets. Six representative IR spectra (Figure 2) from these five locations (all locations, except Grand Coyer, as no IR data are available from that site) show matches with the Fe/Mg smectites[15] that have been previously reported from remote-sensing studies in the same crater[3,5]. We have further confirmed our findings from IR spectroscopic results with the help of LIBS data from the same locations (Figure 3).

Smectite minerals possess structural water, which contributes to the prominent absorption features near the 1.4 and 1.9 μm regions of the reflectance spectra. Overtones of structural OH stretching vibrations and combination tones of water occur near 1.4 μm. Additionally, the 1.9-μm absorption feature results from a combination tone of the fundamental bending and stretching vibrations of the water molecule[16]. Other absorption features due to structural OH combination stretching and bending vibrations occur between the 2.1 and 2.5 μm region[17]. The position and strength of the OH overtone and combination bands (i.e. 1.4- and >2.1-μm features) are functions of relative proportions of Fe, Mg and Al cations in the octahedral site[17]. The 2Fe–OH bending and stretching combination results in an absorption feature near 2.29 μm, whereas for 3Mg–OH combinations, this band tends to appear near 2.31–2.32 μm. A minute absorption feature near 2.4 μm is also related to these bonds[18–20]. The presence of aluminium can be confirmed by a strong 2.21-μm 2Al–OH combination tone in the reflectance spectra of smectites[21,22].

Our observations show that the 1.4-μm absorption feature is centred at 1.41 μm in the IR spectra of the Guillaumes abrasion site (Figure 2). In the spectra from other sites, this feature is either too weak to be detected (because of the abrupt noise in the spectra) or non-existent. All the six IR spectra show a strong 1.9-μm absorption band, attributable to the combination tone of H_2O fundamental bending and stretching vibrations, indicating the presence of structural water in the rocks of the Martian surface. The Guillaumes spectra show the most prominent 1.9-μm feature, centring at ~1.93 μm, with left and right shoulders at ~1.84 and 2.01 μm (Figure 2). However, the same band is easily detectable in other targets (i.e. Lagne, Castillon, Mure and Roubion) as well, with the band centre varying between 1.91 and 1.94 μm, indicating the varying amount of Fe and Mg in the mineral lattice (for the presence of Fe, band centre will tend to occur at lower wavelength and for Mg, it will appear at relatively longer wavelengths)[16]. The 2.29- and 2.32-μm absorption bands are visible in all the spectra, but Castillon and Guillaumes show the prominence of the 2.29-μm features over the 2.32-μm features (Figure 2). For the others, these two bands are either of equal strength or show stronger 2.32-μm features than their shorter-wavelength counterparts. From this observation, we can conclude that the Castillon and Guillaumes site hosts a more Fe-rich variety of smectites than the other sites. The subtle 2.4-μm band is visible in all the spectra, with band centres varying between 2.37- and 2.41-μm (Figure 2). The broad absorption feature centring at 2.5-μm is characteristic of Fe-smectites in general[20]. This band is mainly responsible for the blue slope beyond 2-μm in the smectite spectra.

In this study, the representative mean LIBS spectra from six targets were analysed for their full spectral range (i.e. 243–843 nm). They were further subdivided into the ultraviolet (UV, 243–340 nm), violet (VIO, 380–470 nm), and visible-to-near infra-red (VNIR, 550–843 nm) ranges for a better understanding and representation (Figure 3). The intensity values were not normalized, but were plotted offset from each other for clear visualization. Most of the major elements showed characteristic peaks in the UV range. The presence of Si, Fe and Mg can be easily theorized by their prominent lines in all the spectra (which occur at ~250–265 nm for Si, ~275 nm for Fe and ~280 nm for Mg) (Figure 3). For Lagne and Roubion, the characteristic peak for Al was flat compared to the others, implying that the soils in these two locations have a lower amount of Al than the other locations. All the spectra showed a prominent Ca emission line in the UV and VIO range, but surprisingly, no Ca-minerals could be identified using IR data (as no doublet feature having shorter and longer wavelengths at 2.31 and 2.51 μm respectively, characteristic of carbonate-bearing minerals, were seen). Prominent Na and relatively weaker K emission lines were found in the VNIR range. In all the spectra, a strong O emission line was observed along with a feeble H emission peak, confirming the presence of OH ion in the targets. In this way, the LIBS data also support the presence of Fe-/Mg-smectites

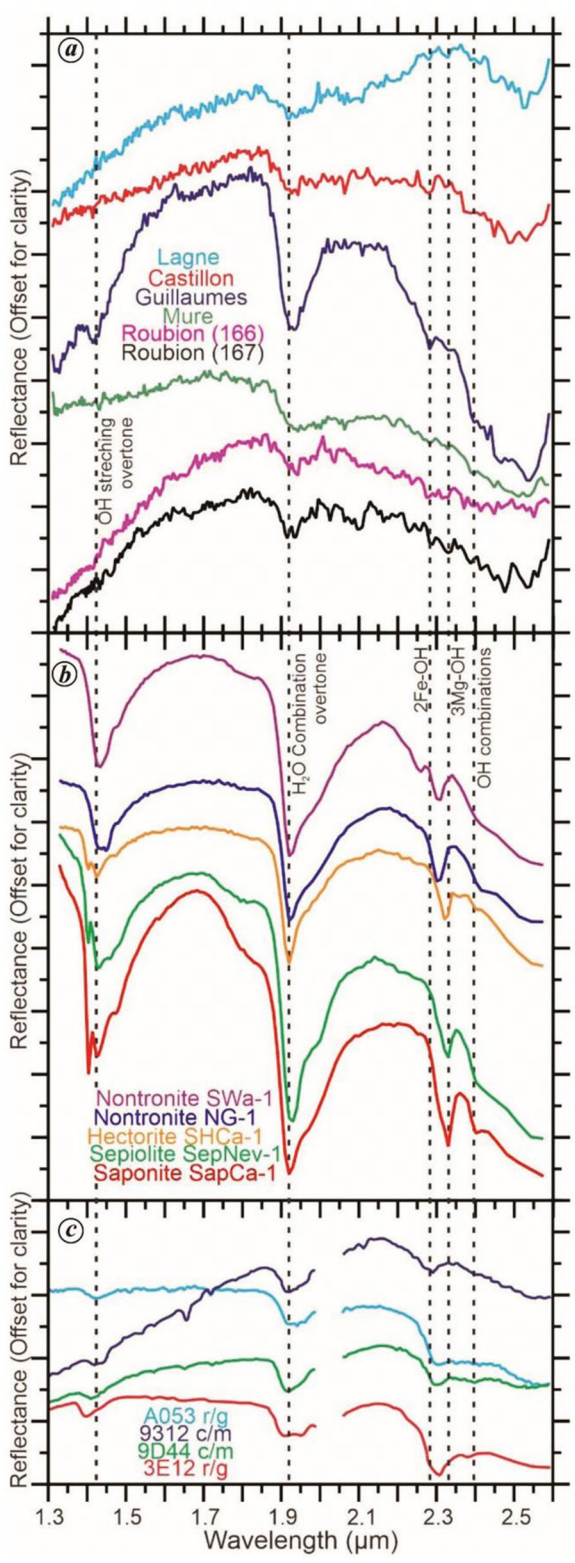

Figure 2. ***a***, Representative IR (1.3–2.6 μm) reflectance spectra collected by the SuperCam instrument from Lagne, Castillon, Guillaumes, Mure and Roubion targets from sol-166 to sol-178. ***b***, USGS Spectral Library spectra for Fe-/Mg-smectites and sepiolite shown for comparison[15]. ***c***, Fe-/Mg-smectite spectra obtained by CRISM instrument from Jezero crater and adjoining places. The spectral identifiers have been mentioned for reference[17]. The dotted lines are drawn at ~1.4, ~1.93, ~2.29, ~2.32 and ~2.4 μm for visual reference.

as deduced from the IR data. This high abundance of Ca can be attributed to previously reported calcium carbonate from this region[3,4,6,23]. The absorption features of Ca-minerals in the reflectance spectra are likely to be masked by the features related to smectites abundant in these samples.

Although the presence of smectites in the Jezero crater is well known from the orbiter[5] and rover[8,9] studies, the unprecedented non-retrieval of the 'Roubion' drill core has shed light on the little-known rheological aspects of these rocks. On Earth, smectites are mostly found as basalt weathering products[24] or fault zone materials[25]. Moreover, using spectroscopic analyses, a few such phyllosilicate- and smectite-bearing horizons from India have already been established as martian analogue sites[24,26–29]. Aqueous alteration of basalts on Mars produces phyllosilicates like nontronite, Fe-rich chlorites, saponite and montmorillonite[30,31]. The widespread occurrence of these minerals in Noachian terrains and scarcity in the later periods (i.e. Hesperian and Amazonian) testify to the switch from a warm–wet to a cold–dry climate, enforcing the termination of hydrous weathering of the primary basaltic crust[32]. Being a weathering/alteration product, smectites and their swelling make the host layers mechanically weak (coefficient of friction <0.25) with a high amount of porosity and

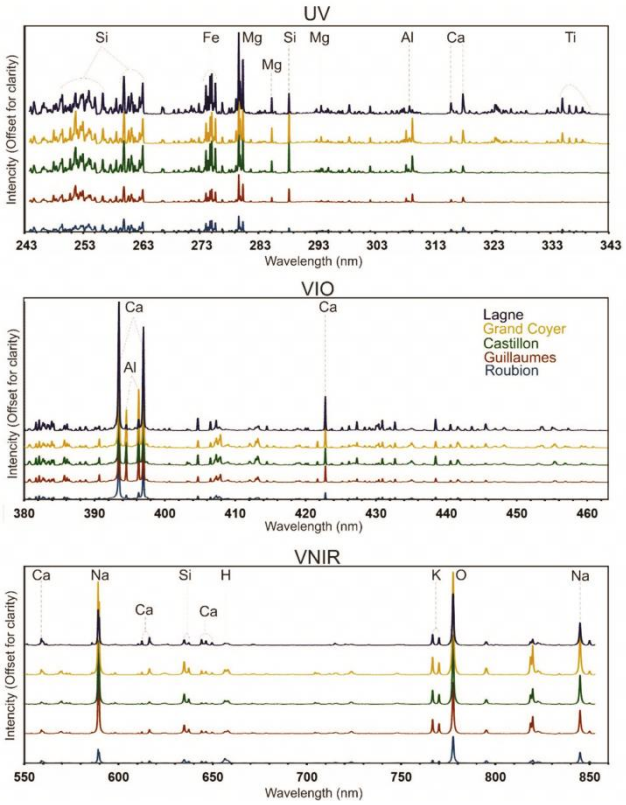

Figure 3. Representative LIBS spectra collected by the SuperCam instrument from Lagne, Grand Coyer, Castillon, Guillaumes and Roubion targets from sol-166 to sol-178. These are further subdivided into the (top) ultraviolet (UV, 243–340 nm), (middle) violet (VIO, 380–470 nm) and (bottom) visible-to-near IR (VNIR, 550–843 nm) ranges for better understanding.

permeability[25,33,34]. Such influence of smectites on the rheological aspects satisfactorily explains the drop of the 'loose' drill core leading to its non-retrieval. The high porosity–permeability, along with the capacity to store huge amounts of water[35], make smectites an excellent host for the preservation of macro- and microscopic biosignatures[36]. For example, several halophilic species of bacteria and archaea have been found in the hyperarid smectite-rich core of the Atacama Desert, Chile[37]. Thus, this identification of smectites in the martian surface and subsurface with the help of the IR spectrometer and LIBS of the SuperCam suite strengthens the hope of finding extinct or extant life on the Red Planet.

1. Farley, K. A. *et al*., Mars 2020 mission overview. *Space Sci. Rev.*, 2020, **216**, 1–41.
2. Schon, S. C., Head, J. W. and Fassett, C. I., An overfilled lacustrine system and progradational delta in Jezero crater, Mars: implications for Noachian climate. *Planet. Space Sci.*, 2012, **67**(1), 28–45.
3. Goudge, T. A., Mustard, J. F., Head, J. W., Fassett, C. I. and Wiseman, S. M., Assessing the mineralogy of the watershed and fan deposits of the Jezero crater paleolake system, Mars. *J. Geophys. Res.–Planets*, 2015, **120**(4), 775–808.
4. Horgan, B. H., Anderson, R. B., Dromart, G., Amador, E. S. and Rice, M. S., The mineral diversity of Jezero crater: evidence for possible lacustrine carbonates on Mars. *Icarus*, 2020, **339**, 113526.
5. Ehlmann, B. L. *et al*., Orbital identification of carbonate-bearing rocks on Mars. *Science*, 2008, **322**(5909), 1828–1832.
6. Tarnas, J. D. *et al*., Orbital identification of hydrated silica in Jezero crater, Mars. *Geophys. Res. Lett.*, 2019, **46**(22), 12771–12782.
7. Voosen, P., Mars rover's sampling campaign begins. *Science*, 2021, **373**(6554), 477.
8. Mandon, L. *et al*., Observing rocks in Jezero crater, Mars: results of the first months of operation of the SuperCam VISIR spectrometer. In Europlanet Science Congress, EPSC2021-534, 2021.
9. Cousin, A. *et al*., Observations of rocks in Jezero landing site: SuperCam/LIBS technique overview of results from the first six months of operations. In Europlanet Science Congress, EPSC2021-644, 2021.
10. Wiens, R. C. *et al*., The SuperCam instrument suite on the NASA Mars 2020 rover: body unit and combined system tests. *Space Sci. Rev.*, 2021, **217**(1), 1–87.
11. Maurice, S. *et al*., The SuperCam instrument suite on the Mars 2020 rover: science objectives and mast-unit description. *Space Sci. Rev.*, 2021, **217**(3), 1–108.
12. Simon, J. I. *et al*., Sampling of Jezero Crater Máaz formation by Mars 2020 Perseverance rover. In Lunar and Planetary Science Conference, 2022, 1294.
13. Murchie, S. *et al*., Compact reconnaissance imaging spectrometer for Mars (CRISM) on Mars reconnaissance orbiter (MRO). *J. Geophys. Res.–Planets*, 2007, **112**, E05S03.
14. PDS Geosciences Node; pds-geosciences.wustl.edu/m2020/urn-nasa-pds-mars2020_supercam/ (accessed on 25 January 2021).
15. Kokaly, R. F. *et al*., USGS Spectral Library Version 7. USGS Data Series 1035, 2017, p. 61.
16. Bishop, J. L., Pieters, C. M. and Edwards, J. O., Infrared spectroscopic analyses on the nature of water in montmorillonite. *Clay Clay Miner.*, 1994, **42**, 702–716.
17. Ehlmann, B. L., *et al*., Identification of hydrated silicate minerals on Mars using MRO-CRISM: geologic context near Nili Fossae and implications for aqueous alteration. *J. Geophys. Res.*, 2009, **114**, E00D08.
18. Clark, R. N. *et al*., High spectral resolution reflectance spectroscopy of minerals. *J. Geophys. Res.*, 1990, **95**, 12653–12680.
19. Frost, R. L., Kloprogge, J. T. and Ding, Z., Near-infrared spectroscopic study of nontronites and ferruginous smectite. *Spectrochim. Acta A*, 2002, **58**(8), 1657–1668.
20. Bishop, J. L., Murad, E. and Dyar, M. D., The influence of octahedral and tetrahedral cation substitution on the structure of smectites and serpentines as observed through infrared spectroscopy. *Clay Miner.*, 2002, **37**, 617–628.
21. Bishop, J., Madejova, J., Komadel, P. and Froschl, H., The influence of structural Fe, Al, and Mg on the infrared OH bands in spectra of dioctahedral smectites. *Clay Miner.*, 2002, **37**, 607–616.
22. Bishop, J. L. *et al*., Phyllosilicate diversity and past aqueous activity revealed at Mawrth Vallis, Mars. *Science*, 2008, **321**, 830–833.
23. Zastrow, A. M. and Glotch, T. D., Distinct carbonate lithologies in Jezero crater, Mars. *Geophys. Res. Lett.*, 2021, **48**(9), e2020GL092365.
24. Bhattacharya, S. *et al*., Jarosite occurrence in the Deccan Volcanic Province of Kachchh, western India: spectroscopic studies on a Martian analog locality. *J. Geophys. Res.–Planets*, 2016, **121**(3), 402–431.
25. Kameda, J. *et al*., Fault weakening caused by smectite swelling. *Earth Planets Space*, 2019, **71**(1), 1–7.
26. Parthasarathy, G. *et al*., Ferrous saponite from the Deccan Trap, India, and its application in adsorption and reduction of hexavalent chromium. *Am. Mineral.*, 2003, **88**(11–12), 1983–1988.
27. Saikia, B. J. and Parthasarathy, G., Fourier transform infrared spectroscopic characterisation of kaolinite from Assam and Meghalaya, Northeastern India. *J. Mod. Phys.*, 2010, **1**(4), 206–210.
28. Parthasarathy, G. and Sarkar, P. K., High pressure temperature studies of phyllosilicates from the Deccan Trap, India: implications to Martian mineralogy and near subsurface processes. In Lunar and Planetary Science Conference, Texas, USA, 2014, 1326.
29. Mitra, S. *et al*., Jarosite precipitation from acidic saline waters in Kachchh, Gujarat, India: an appropriate Martian analogue? In AGU Fall Meeting, San Francisco, USA, 2014, P41A-3891.
30. Bibring, J. P. *et al*., Global mineralogical and aqueous Mars history derived from OMEGA/Mars Express data. *Science*, 2006, **312**(5772), 400–404.
31. Zolotov, M. Y. and Mironenko, M. V., Early alteration of matrices in parent bodies of CI/CM carbonaceous chondrites: kinetic–thermodynamic modeling. In Lunar and Planetary Science Conference, Texas, USA, 2008, 1998.
32. Carr, M. H. and Head, J. W., Acquisition and history of water on Mars. In *Lakes on Mars* (eds Grin, E. A. and Cabrol, N. A.), Elsevier, 2010, pp. 31–67.
33. Vrolijk, P., On the mechanical role of smectite in subduction zones. *Geology*, 1990, **18**(8), 703–707.
34. Saffer, D. M., Frye, K. M., Marone, C. and Mair, K., Laboratory results indicating complex and potentially unstable frictional behavior of smectite clay. *Geophys. Res. Lett.*, 2001, **28**(12), 2297–2300.
35. DePasquale, B. M. and Jenkins, D. M., The upper-thermal stability of an iron-rich smectite: implications for smectite formation on Mars. *Icarus*, 2022, **374**, 114816.
36. Yamashita, S. *et al*., Iron-rich smectite formation in subseafloor basaltic lava in aged oceanic crust. *Sci. Rep.*, 2019, **9**(1), 1–8.
37. Azua-Bustos, A. *et al*., Inhabited subsurface wet smectites in the hyperarid core of the Atacama Desert as an analog for the search for life on Mars. *Sci. Rep.*, 2020, **10**, 19183.

ACKNOWLEDGEMENTS. S.S. thanks the Department of Science and Technology, Government of India, for funding his doctoral research work through INSPIRE scheme (fellowship registration number: IF170-664). We thank PDS Geosciences Node for providing the data, and Dr S. Suresh Babu (handling editor) and two anonymous reviewers for their useful comments and suggestions that helped improve the manuscript.

Received 2 February 2022; revised accepted 5 May 2022

doi: 10.18520/cs/v123/i1/93-96